

Fatigue Behavior of Reinforced Concrete Beams Strengthened with Different FRP Laminate Configurations

by R. Gussenhoven and S.F. Breña

Synopsis: This paper presents testing results of thirteen small-scale beams strengthened using carbon fiber-reinforced polymer composites tested under repeated loads to investigate their fatigue behavior. The beams were strengthened using different thicknesses and widths of composite laminates to identify parameters that would generate different failure modes. Two predominant fatigue failure modes were identified through these tests: fatigue fracture of the steel reinforcement with subsequent debonding of the composite laminate, or fatigue fracture of the concrete layer below the tension reinforcing steel (concrete peel off). Test results indicate that peak stress applied to the reinforcing steel in combination with composite laminate configuration are the main parameters that affect the controlling failure mode. Tests on large-scale components are required to verify the results presented in this paper.

Keywords: carbon fiber-reinforced polymers; fatigue loading; reinforced concrete; strengthening

614 Gussenhoven and Breña

Maj. Richard Gussenhoven is an Instructor in the Department of Mathematical Sciences and Assistant Director for the Center of Data Analysis and Statistics in the U.S. Military Academy at West Point. He received his MS degree at the University of Massachusetts Amherst in 2004.

Sergio F. Breña is an Assistant Professor at the University of Massachusetts Amherst. He is a member of ACI Committee 440 – Fiber Reinforced Polymer, ACI 374 – Performance Based Seismic Design, ACI-ASCE 445 – Shear and Torsion, and ACI 369 Repair and Rehabilitation.

INTRODUCTION

Strengthening existing reinforced concrete structures using composites is an accepted technology that is being increasingly used in a wide variety of applications. This technology is particularly promising for bridge applications because of the large number of existing bridges that need repair or replacement. Additionally some bridge strengthening applications are required because of an increase in vehicle weight over the years (Breña et al. 2003). As a result, old bridges designed using lower live-load models require strengthening to meet current load standards.

Carbon fiber-reinforced polymer (CFRP) composites have been investigated to strengthen existing older bridges. Many of the studies available in the literature have been conducted on specimens loaded statically with comparatively few studies performed using fatigue loading. An understanding of the factors affecting the fatigue performance of strengthened beams is required to develop appropriate design guidelines for bridge applications.

RESEARCH OBJECTIVES

The primary objective of this research study was to identify the failure modes that occur in beams strengthened using CFRP composites and loaded under repeated loads. Parameters including laminate width and thickness, amplitude of cyclic loading, and pre-existing damage in the beams were investigated.

DESCRIPTION OF LABORATORY SPECIMENS

Thirteen small-scale beams were fabricated and tested to investigate the effects of various parameters including composite laminate configuration on their fatigue performance. Two of these specimens were used as control specimens, and the rest were strengthened using carbon fiber-reinforced polymer (CFRP) laminates. The CFRP laminate configuration varied on the strengthened specimens within their respective specimen group. Details of the strengthening configurations corresponding to each specimen group are given in the following sections.

Specimen Geometry and Reinforcement

The laboratory specimens had a 102 by 102 mm cross-section with a 914 mm total length. Longitudinal reinforcement consisted of 2 – #10M reinforcing bars with a nominal yield stress of 410 MPa on the tension and compression sides of the beam. Transverse reinforcement consisted of 16 stirrups at a 51 mm spacing placed within the shear spans constructed using gage D4 deformed wire. The transverse reinforcement was designed to avoid shear failures of the beams after flexural strengthening. Concrete clear cover was 13 mm from the exterior face of the beam to the transverse reinforcement on all faces (Figure 1).

SPECIMEN GROUPS AND STRENGTHENING CONFIGURATIONS

Specimens were fabricated in three groups depending on casting date. The first two groups (A and B) consisted of five beams, and the third group (group C) consisted of three beams. Details of each specimen group are discussed below. Table 2 presents a summary of the experimental parameters varied in the three groups. The primary experimental parameter in each group was different as discussed in the following sections. Eleven of the specimens were strengthened using a commercially available CFRP strengthening system (Master Builders 1998 MBrace C-130). Measured material properties used in this research are presented in Table 1.

The CFRP laminates were bonded on the tension face of the beams and terminated 25 mm from the face of each support, resulting in a total laminate length of 762 mm. The laminates were formed by wet layup and cured at ambient temperature for at least seven days before testing. The laminates were either 89 or 51 mm wide, and were formed using one or two plies depending on the specimen group. No supplemental anchorage was used along the composite laminates to allow the possibility of debonding as a failure mode after repeated loading. The typical strengthening configuration is shown in Figure 2.

Group A

Strengthened beams in this group were strengthened using a one-ply, 89-mm wide laminate. The primary variable for these specimens was the loading amplitude so all specimens had the same laminate configuration. A high load amplitude, close to the expected fatigue limit of the reinforcing steel, was used when testing these specimens to investigate any favorable effects that the CFRP laminates might have in the fatigue life of the beams as a result of increased stiffness, reduction of crack width, and larger crack spacing at service loads. All these attributes have been reported in beams strengthened with composite laminates.

Two of the five beams in group A were used as control specimens: one unstrengthened specimen and one strengthened specimen. The unstrengthened specimen was tested using repeated loading that generated peak stresses in the tension steel equal to

616 Gussenhoven and Breña

80% of the yield stress. The strengthened control beam contained the same composite configuration as the rest of the specimens in this group, and was tested statically to failure to provide a static-load baseline for the repeated load tests.

Group B

Beams in group B were strengthened using CFRP laminates of equal width (51 mm) but different thickness. The effect of composite thickness on the fatigue behavior of the specimens was the primary experimental parameter in this group. The applied load was increased in beams strengthened using 2-ply CFRP laminates in order to generate the same peak stress in the reinforcing steel as beams with only 1-ply laminates. Laminate area in beams strengthened with a 1-ply laminate was approximately 57% of the area in group A specimens, and beams with 2-ply laminates had approximately 14% more area than beams in group A. The laminate surface contact area in these beams was only equal to 57% of the area provided in group A specimens. Interface stresses in beams with 1-ply laminates in group B would be theoretically equal to those in beams in group A. Because of higher thickness and smaller contact surface in specimens with 2-ply laminates, interface stresses would be twice as large as those generated in beams in group A at equal laminate strains.

Group C

The three beams in group C were subjected to 500,000 cycles of repeated loads generating a stress equal to 50% of the yield stress in the tensile reinforcement prior to strengthening. These beams were subsequently strengthened using identical CFRP configurations to those used in beams with 1-ply laminates from group B. The loading protocol after strengthening was designed to produce the same stress levels as those generated in the companion specimens in group B.

TEST SETUP, INSTRUMENTATION, AND LOADING PROTOCOL

All members were subjected to 4-point bending using an 8500 Instron testing machine. Load was measured using a 50 kN load cell mounted to the machine piston. The specimens were supported on plates and rollers, which simulated a simply supported condition and rested on a stiff beam mounted on the testing machine load frame. A picture of the experimental setup is shown in Figure 3.

Beam deflections were measured using linear potentiometers positioned at mid-span and at support centerlines to account for flexibility of the supporting beam. A linear variable displacement transducer (LVDT) integral to the hydraulic actuator was used to measure the deflection at the load points. In order to measure the strain profile across the cross section, each beam was instrumented at the mid-span with strain gages to measure the strain on the tension reinforcement, the compression face, and the CFRP laminate for the strengthened beams. Strain gages were applied to both reinforcing bars on the tension side of the beam with a protective coating to prevent damage during concrete placement. Two strain gages were positioned on the compression face at mid-span to measure concrete strains. In beams strengthened with CFRP laminates, two strain

gages were applied at mid-span 13 mm from the exterior edge of the CFRP laminate (Figure 4).

Repeated Load Protocol and Data Acquisition

Repeated loads were applied using a sinusoidal variation between minimum and maximum values. A minimum load of 2.7 kN was selected to avoid shifting of the beams with cycling while generating stresses that could be considered representative of dead loads in beams. The maximum load was calculated to generate specified stress levels in the tension reinforcement as a fraction of the nominal yield stress (60, 70, or 80% of nominal yield stress). A peak stress in the reinforcement equal to 60% of yield was intended to represent service-load stress conditions that would be typically encountered in practice. A peak reinforcing bar stress of 80% of yield represents the upper strengthening limit recommended by ACI Committee 440 (2002). The load frequency used for all repeated-load tests was approximately 4-Hz.

Loading was stopped periodically after reaching predetermined numbers of cycles to inspect beams for damage and acquire data during a low-frequency cycle. The data acquisition cycle consisted of a full cycle of loading between the minimum and maximum load values while acquiring deformation and strain data.

EXPERIMENTAL RESULTS

Damage progression in the specimens was monitored visually by examining crack growth and formation of new cracks during testing. Most of the new cracks or growth of existing cracks occurred during the early cycles of loading (up to 20,000). Subsequently, observed damage in the beams did not increase substantially. In many cases, no indications of imminent failure were observed, especially in beams where the reinforcing bars failed by fatigue fracture. The observed failure modes and the associated damage progression are described in the next sections. Deflection and strain measurements as additional damage indicators are also presented afterward.

Observed Failure Modes

The observed failure modes were dependent on the selected peak stress levels in the tension reinforcement and the configuration of the CFRP laminates. Specimens that withstood at least 2 million cycles of loading without failing were considered to have an infinite fatigue life and were subsequently tested statically to failure. These specimens did not exhibit any strength degradation compared with the control specimen after cycling. Table 3 lists the steel reinforcement peak stress, the applied stress range, the number of cycles to failure, and the associated failure modes observed during the tests.

Specimens cycled at peak stresses equal to 70 or 80% of the yield stress exhibited one of two failure modes depending on stress amplitude and CFRP laminate configuration. Failure modes in these beams were characterized by fatigue fracture of the reinforcement with subsequent debonding of the CFRP laminate or failure of the concrete cover along the bottom reinforcement. Figure 5 shows a specimen that exhibited steel

618 Gussenhoven and Breña

fracture and subsequent debonding of the CFRP laminate. In this type of failure mode, after the reinforcing bars fractured the excess force generated in the CFRP laminate triggered loss of bond between the laminate and concrete surface. These beams showed no visible indication of distress prior to fracture of the reinforcement, as the cracks had stabilized and ceased to grow in length.

Beams that exhibited failure along the concrete cover were characterized by visible indications of damage as loading progressed. Typically a crack formed at the end of the CFRP laminate during early loading cycles (Figure 6a and Figure 7a) and later propagated along a plane just below the tension reinforcing bar level. The end crack propagated sometimes in the form of diagonal cracks within the beam shear span causing severe crack widening to occur within this region (Figure 6b).

Global Behavior – S-N Plots

Stress range is widely recognized as having a major influence in the fatigue life of metals. A number of fatigue life models for steel reinforcing bars used in concrete applications have been published in the past. From a series of reinforcing bars repeated tension tests, Helgason and Hanson (1974) proposed the following relationship to determine fatigue life of reinforcing bars:

$$\log N = 6.969 - 0.0055f_r \quad (1)$$

where N is the number of cycles to failure and f_r is the applied stress range in MPa. Fatigue fracture of reinforcing bars embedded in concrete typically occurs in the proximity of concrete cracks that form as a result of loading. As a result of a study to examine the effects of concrete on fatigue life of reinforcement, Moss (1982) developed a fatigue life model based on the results of bending tests of reinforcing bars embedded in concrete. The following relationship was developed from a regression analysis of test data:

$$N f_r^m = K \quad (2)$$

where m represents the inverse slope of the stress range – number of cycles curve (S-N curve) = 8.7, and K is a constant calibrated to the test data = 0.59×10^{27} to represent the mean minus two standard deviations curve. ACI Committee 215 (1997) recommends that the maximum stress range in reinforcing bars in non-prestressed flexural members be limited to the following relationship to achieve an infinite fatigue life:

$$f_r = 161 - 0.33f_{\min} \quad (3)$$

where f_{\min} is equal to the minimum (permanent) stress acting in the reinforcement.

Test data points of the strengthened beams in this study are plotted along with Equations 1 to 3 in the S-N plot shown in Figure 8. It can be observed that the majority of the data points generated in this study fall close to the Helgason-Hanson fatigue life

model. Only two data points fall significantly to the left of Helgason-Hanson model, indicating that these specimens had a lower fatigue life than predicted by this model. Both specimens failed by concrete cover failure, which explains the poor correlation with the model. The apparent slope of data points from the three beam series tested in this research study appears to follow the slope of the model proposed by Moss (1982). This result should not be surprising since the majority of the specimens were controlled by fatigue fracture, which would be consistent with the failure mode captured by this model.

Test results reported by Papakonstantinou et al. (2001) are also shown in Figure 8. These researchers conducted tests of unstrengthened beams and strengthened beams using glass fiber-reinforced composites. The reported failure mode for all their tests consisted of steel fatigue fracture. It should be pointed out, however, that for all the strengthened beams in their study the FRP laminates extended past the supports so FRP debonding was restrained by clamping from support plates near the beam ends. Data points from the tests by Papakonstantinou consistently reached higher fatigue lives than the beams reported in this paper. Data from unstrengthened specimens consistently lie to the right of the Helgason-Hanson model, and there is no clear evidence of an increase in fatigue life from the use of composite laminates. This result is in contrast with observations from other researchers that reported that fatigue life of FRP-strengthened concrete beams was higher than life of companion unstrengthened specimens (Barnes and Mayes 1999).

The influence of laminate geometric parameters (width and thickness) on fatigue life was investigated by plotting the ratio of laminate force to laminate width or laminate thickness as a function of number of cycles to failure. Only specimens that failed in fatigue were included in this study. Only two specimens were strengthened using twice the laminate thickness than the rest (Table 2), and only one of those failed in fatigue. Because of this, conclusive evidence of any effect of laminate thickness on fatigue life could not be obtained in this research.

Laminate width, on the other hand, seemed to have a definite influence on fatigue life of the specimens. Figure 9 shows plots of laminate force as a function of number of cycles to failure. The test data was separated into two groups depending on the laminate width used: 89 mm or 51 mm. As Figure 9 (a) indicates, the two specimens where the highest laminate force was developed during the first loading cycle eventually failed by concrete clear cover peel off. Furthermore, the data follow two distinct trends depending on laminate width, as shown by best-fit lines drawn through the data points. The ratio of laminate force to laminate width was used to generate the data shown in Figure 9 (b). It can be seen that, to achieve comparable increases in fatigue life, a higher decrease in laminate force per unit width was required in specimens with 51-mm laminates compared with those with 89-mm laminates. Fatigue life in specimens strengthened using 51-mm wide laminates increased approximately 3 times (from 150,000 to 440,000 cycles) for a laminate unit force decrease of approximately 0.13 kN/mm, while specimens strengthened with 89-mm laminates had approximately a six-fold increase in fatigue life (from 130,000 to 779,000) for a laminate unit force decrease of only 0.03 kN/mm. This behavior could be attributed to wider laminates being able to

620 Gussenhoven and Breña

restrain crack opening more efficiently than narrower laminates, therefore delaying fatigue failure of reinforcing steel.

Deflection and Strain Variation with Cycling

Increase in deflection was used as another measure of damage accumulation with cycling. Mid-span deflection increased markedly during the first 10 to 20 thousand cycles as new cracks formed and existing cracks extended. Crack formation and growth resulted in a reduction in effective moment of inertia of the specimens, which caused an increase in deflections. After approximately 20 thousand cycles deflections did not increase significantly for the majority of the specimens except those failing by concrete cover peel off. Figure 10 shows the midspan deflection comparison between a specimen that failed by steel fatigue fracture (specimen B-1-2-70) and one that failed by concrete peel off (specimen B-2-2-70). Mid-span deflection in specimen B-2-2-70 increased significantly after 100 thousand cycles of loading as a result of initiation of cover peel off. Contrastingly there was only a slight increase in deflection in specimen B-1-2-70 after initial cycling up to approximately 20 thousand cycles. The behavioral trends observed in these two specimens are also representative of behavior observed in other specimens in this research.

Strains in the specimens were expected to follow a similar variation as deflection. Figure 11 shows the strain variation in the concrete, steel, and CFRP laminates as a function of number of load cycles in specimen B-1-2-70. In this figure negative values represent compressive strains (concrete strains) and positive values represent tensile strains (steel and CFRP strains). The figure indicates that concrete and steel strains follow the expected variation, that is, significant strain increase during the first few thousand cycles of loading with little increase afterwards. Contrastingly one of the CFRP strain gages exhibited a marked reduction, particularly after 150 thousand cycles of loading. These types of variations were not uncommon in other specimens so definitive conclusions about damage progression could not be made using strain gage data. From these results, it was found that displacement measurements provided the most reliable indicator of damage progression in these tests.

SUMMARY AND CONCLUSIONS

Thirteen small-scale beams were strengthened using CFRP composites and tested under fatigue loading. The effect of composite configuration on the fatigue failure mode was investigated through these tests. Three values of peak stress applied to the tension reinforcing steel, which generated different stress ranges during application of repeated loads, were studied. Two primary fatigue failure modes were identified in these studies: fatigue fracture of reinforcing steel for beams subjected to moderate peak stresses (up to 70% of yield), or fatigue fracture of the concrete cover below the reinforcing steel for beams subjected to high steel stresses (between 70 and 80% of yield) and stiff composite laminates. The fatigue test results could be predicted reasonably well with an existing fatigue life model proposed for reinforced concrete beams. Wider laminates were more effective than narrower laminates to increase fatigue life of strengthened beams. Beam deflection was considered a more reliable indicator of damage progression

than measured strains in the beams. Additional tests in larger beams are needed to verify these tests results and identify other parameters that might affect fatigue behavior (shear span, existing reinforcement ratio).

REFERENCES

ACI Committee 215 (1997). *Considerations for Design of Concrete Structures Subjected to Fatigue Loading*, American Concrete Institute, ACI 215R-74 (Reapproved 1997), Farmington Hills, MI, 24 pp.

ACI Committee 440 (2002). *Guide for the Design and Construction of Externally Bonded FRP Systems for Strengthening Concrete Structures*, American Concrete Institute, ACI 440.2R-02, Farmington Hills, MI, 45 pp.

Barnes, R. A. and Mayes, G. C. (1999). "Fatigue Performance of Concrete Beams Strengthened with CFRP Plates." *Journal of Composites for Construction*, Vol. 3, No. 2, May, pp. 63-72.

Breña, S.F., Wood, S.L., and Kreger M.L. (2003). "Full-scale Tests of Bridge Components Strengthened using Carbon Fiber-Reinforced Polymer Composites." *ACI Structural Journal*, Vol. 100, No. 6, November-December 2003, pp. 775-784.

Helgason T. and Hanson J.M. (1974). "Investigation of Design Factors Affecting Fatigue Strength of Reinforcing Bars – Statistical Analysis." *Abeles Symposium on Fatigue of Concrete*, SP-41, American Concrete Institute, Farmington Hills, MI, pp. 107-138.

Master Builders, Inc. (1998). *MBraceTM Composite Strengthening System-Engineering Design Guidelines*, Cleveland, OH, 1998.

Moss, D.S. (1982). "Bending Fatigue of High-yield Reinforcing Bars in Concrete." *TRRL Supplementary Rep. 748*, Transport and Road Research Laboratory, Crowthorne, U.K.

Papakonstantinou, C.G., Petrou, M.F., and Harries, K.A. (2001). "Fatigue Behavior of RC Beams Strengthened with GFRP Sheets." *Journal of Composites for Construction*, ASCE, Vol. 5, No. 4, pp. 246-253.

622 Gussenhoven and Breña

Table 1 — Measured material properties

Parameter	Value
Concrete compressive strength, MPa	Group A = 28.3, Group B = 29.9, Group C = 29.0
Steel yield stress, MPa	420
CFRP tensile strength, MPa	3800
CFRP modulus of elasticity, GPa	260
CFRP rupture strain	0.0146

Table 2 — Specimen Matrix

Specimen	No. of Plies	CFRP Width	CFRP thickness [†]	f_t/f_y^*
		(mm)	(mm)	
A-1-4-Mono	1	89	0.17	--
A-Control	0	0	0	--
A-1-4-80	1	89	0.17	0.80
A-1-4-70	1	89	0.17	0.70
A-1-4-60	1	89	0.17	0.60
B-1-2-80	1	51	0.17	0.80
B-1-2-70	1	51	0.17	0.70
B-1-2-60	1	51	0.17	0.60
B-2-2-70	2	51	0.34	0.70
B-2-2-60	2	51	0.34	0.60
C-1-2-80	1	51	0.17	0.80
C-1-2-70	1	51	0.17	0.70
C-1-2-60	1	51	0.17	0.60

[†] Thickness based on fiber properties.

* Ratio of applied tension steel stress to nominal yield stress.

Specimen Designation Key

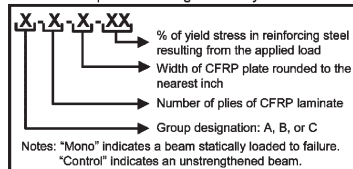


Table 3 — Summary of load parameters and failure modes

Specimen	Peak Stress, MPa	Stress Range, MPa	No. of cycles to failure	Failure mode
A-Control	368	310	183,674	Fatigue of Reinforcement
A-1-4-80	332	295	131,619	Concrete Clear Cover Peel Off
A-1-4-70	316	272	287,594	Fatigue of Reinforcement followed by CFRP Debonding
A-1-4-60	265	224	778,734	Fatigue of Reinforcement and Concrete Cover Peel Off
B-1-2-80	347	300	290,307	Fatigue of Reinforcement followed by CFRP Debonding
B-1-2-70	309	268	336,873	Fatigue of Reinforcement followed by CFRP Debonding
B-1-2-60	283	236	4,000,000+	Statically Loaded to Failure after 4 Million Cycles
B-2-2-70	328	270	150,000	Concrete Clear Cover Peel Off
B-2-2-60	256	199	2,000,000+	Statically Loaded to Failure after 2 Million Cycles
C-1-2-80U	220	175	500,000	No Failure
C-1-2-70U	229	182	500,000	No Failure
C-1-2-60U	193	137	500,000	No Failure
C-1-2-80S	320	326	326,775	Fatigue of Reinforcement followed by CFRP Debonding
C-1-2-70S	298	226	440,193	Fatigue of Reinforcement followed by CFRP Debonding
C-1-2-60S	227	189	4,000,000+	Statically Loaded to Failure after 4 Million Cycles

624 Gussenhoven and Breña

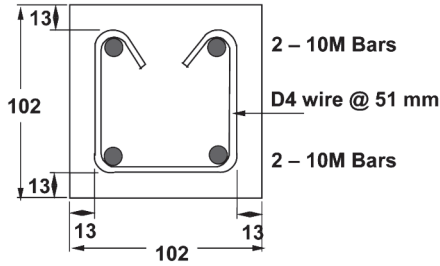
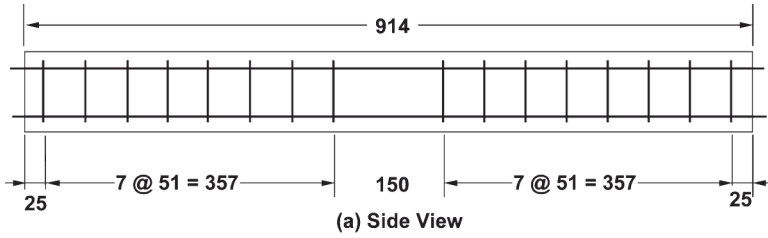


Figure 1 — Specimen geometry and reinforcement

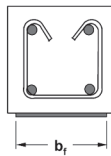
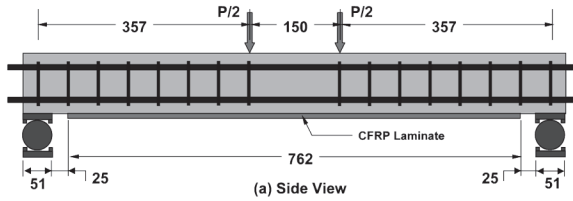


Figure 2 — CFRP strengthening configuration



Figure 3 – Experimental setup used in the tests

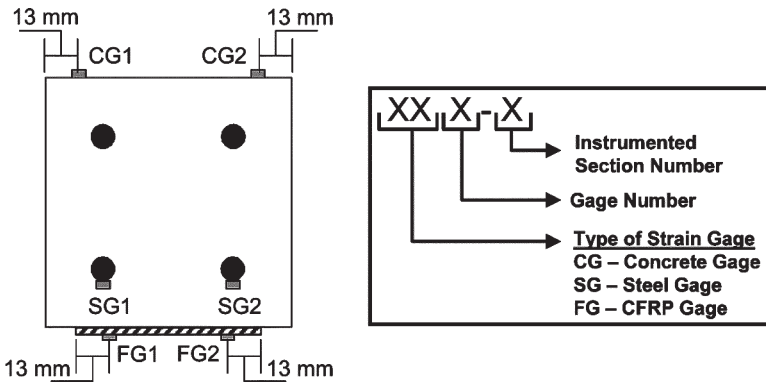


Figure 4 – Specimen Instrumentation

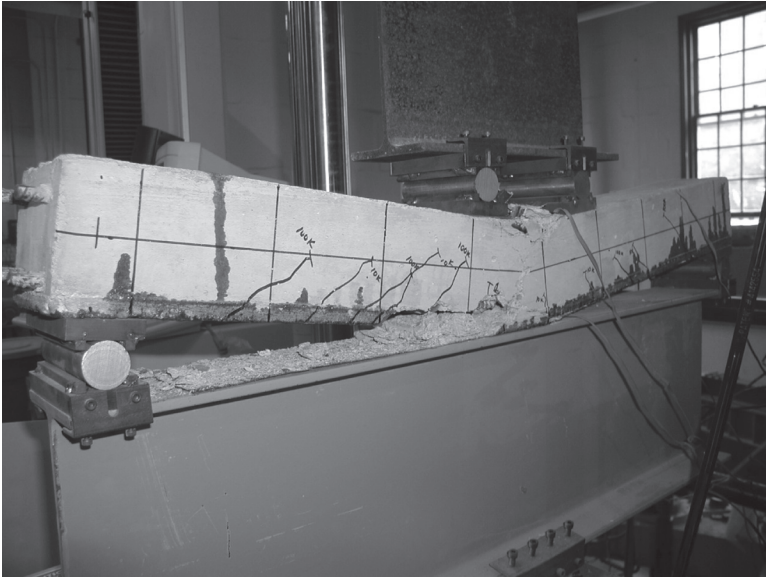
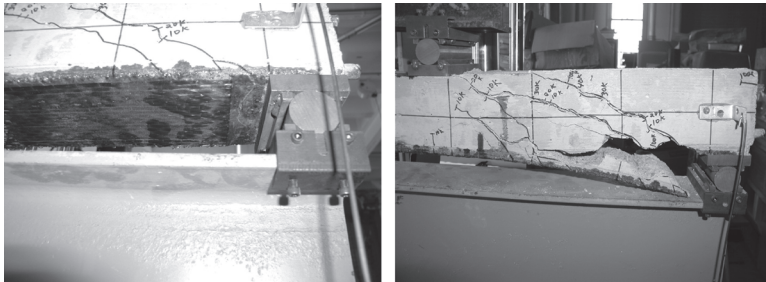


Figure 5 — CFRP debonding after fatigue fracture of reinforcing steel (Specimen A-1-4-70)



(a)

(b)

Figure 6 — Damage progression in specimen A-1-4-80; (a) Formation of crack at end of CFRP laminate, and (b) extension of end crack along concrete cover and shear span

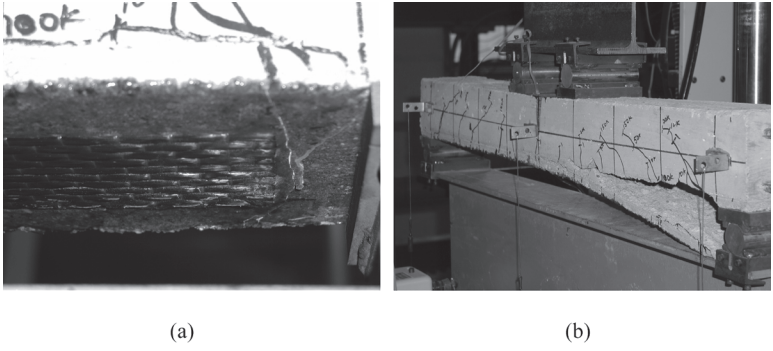


Figure 7 — Damage progression in specimen B-2-2-70; (a) crack initiation at end of CFRP laminate, and (b) concrete cover failure

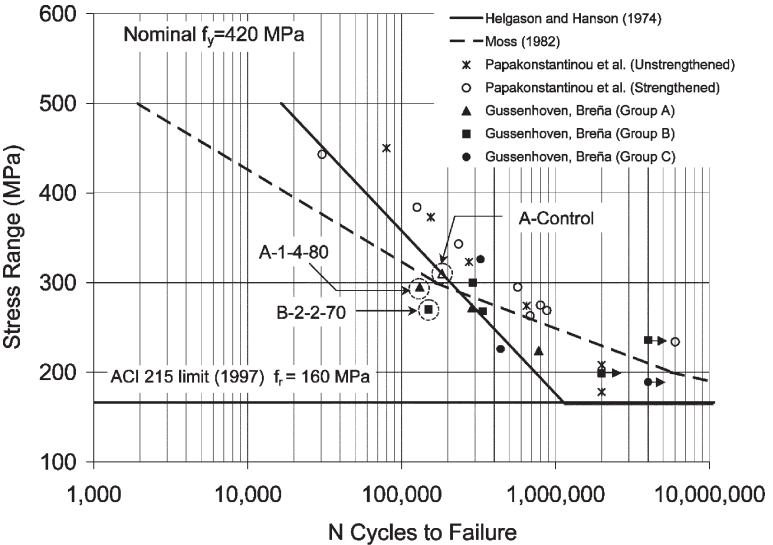
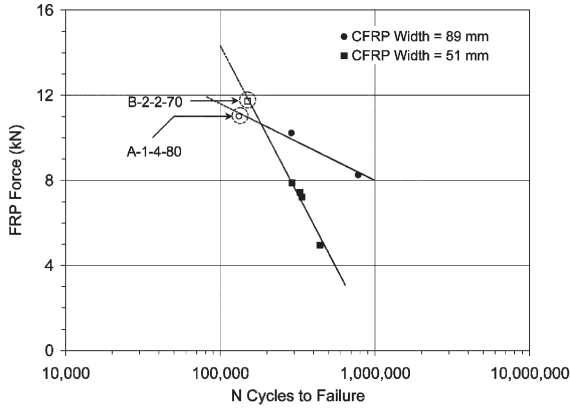
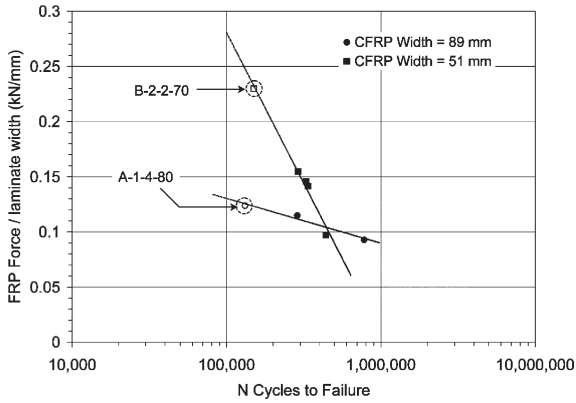


Figure 8 — Comparison between fatigue life models and results of tests

628 Gussenhoven and Breña

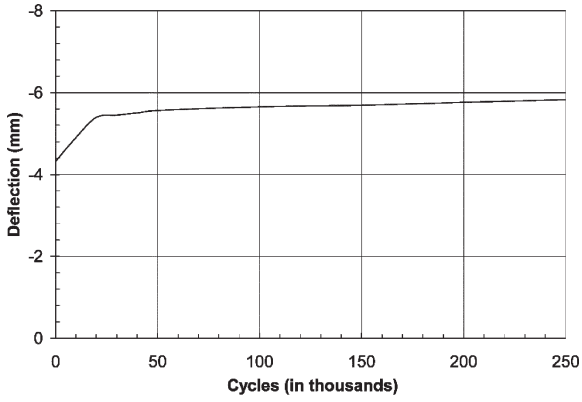


(a) Fatigue life as a function of CFRP laminate force in first cycle

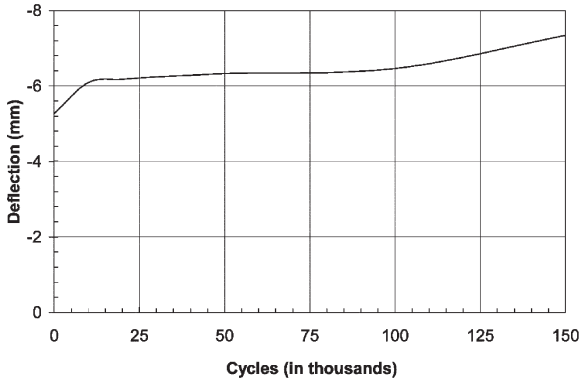


(b) Fatigue life as a function of CFRP laminate force/width in first cycle

Figure 9 — Effect of laminate width on fatigue life



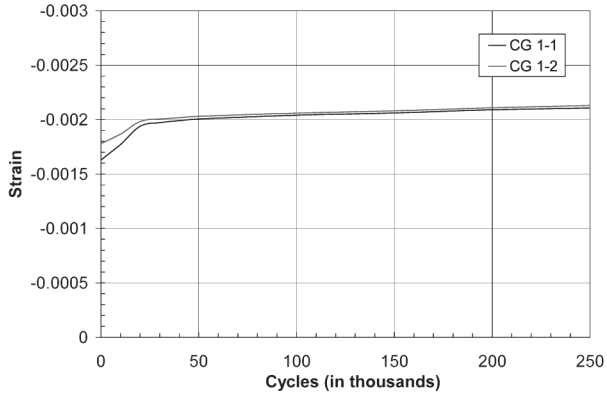
(a) Specimen B-1-2-70



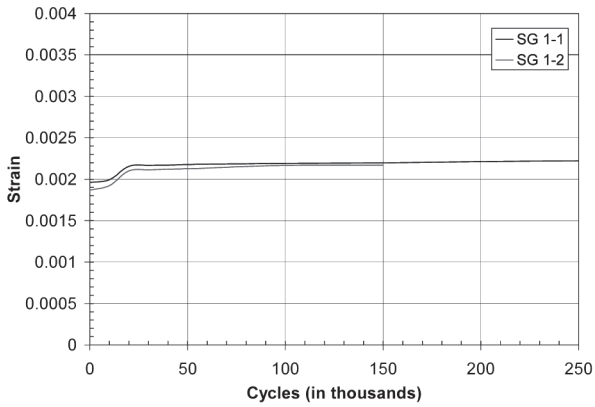
(b) Specimen B-2-2-70

Figure 10 — Variation of mid-span deflection with number of applied cycles

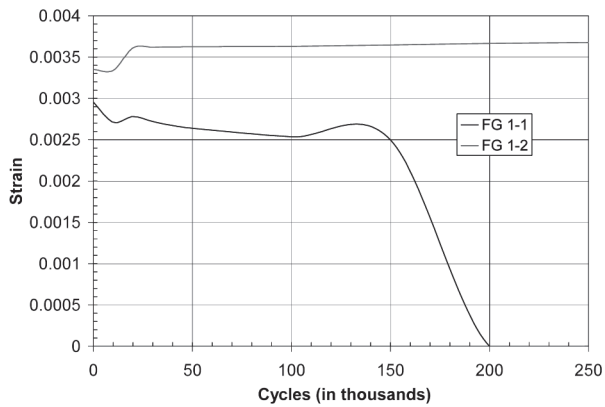
630 Gussenhoven and Breña



(a) Concrete strains



(b) Steel Strains



(c) CFRP Strains

Figure 11 — Strain variation with cycling (Specimen B-1-2-70)